International Journal for Quality Research 7(4) 605–622
ISSN 1800-6450

María Teresa Carot
Aysun Sagbas[1]
José María Sanz

Article info:
Received 19 July 2013
Accepted 20 November 2013

UDC – 65.012.7

A NEW APPROACH FOR MEASUREMENT OF THE EFFICIENCY OF C_{pm} AND C_{pmk} CONTROL CHARTS

Abstract: *Process capability analysis is a very effective way for improving process quality by relating process variation to customer requirements. It compares the output of a process to the specification limits by using process capability indices (PCIs). PCIs provide numerical measures on whether a process conforms to the defined manufacturing capability prerequisite. In this paper, a new approach based on non-central Chi-Square, ω and φ distributions is presented to design the capability control charts. The main purpose of this work is to investigate the efficiency of the proposed control charts comparing with the traditional control charts. The advantage of using the proposed capability control charts is that, the practitioner can monitor the process mean and the process variability by looking at one chart. Moreover the proposed capability control charts are easily appended to* $\bar{X} - R$ *control chart and provide judgments considering the ability of a process to meet requirements. To demonstrate* the *applicability of the proposed approach an illustrative example is conducted.*

Keywords: *Statistical process control, process monitoring, control chart,* C_{pm}, C_{pmk}

1. Introduction

During the last decade, numerous process capability indices, including C_p, C_{pk}, C_{pm} and C_{pmk} have been widely used to provide numerical measures on process potential and performance in manufacturing industries requiring very low fraction of nonconformities. Based on analyzing the *PCIs*, production practitioners can trace and improve the process. By doing this, the quality level of the process can be enhanced and the requirements of the customers can be satisfied. Assuming that, the process measurement follows a normal distribution closely, the following commonly used capability indices were defined as (1):

$$C_p = \frac{T_2 - T_1}{6 \cdot \sigma}$$
$$C_{pk} = min\left(\frac{T_2 - \mu}{3 \cdot \sigma}, \frac{\mu - T_1}{3 \cdot \sigma}\right)$$
$$C_{pm} = \frac{T_2 - T_1}{6 \cdot \sqrt{\sigma^2 + (\mu - T)^2}} \quad (1)$$

Where T_2 is the upper specification limit, T_1 is the lower specification limit, μ is the process mean, σ is the process standard deviation and T is the target value, predetermined by the product designer.

[1]Corresponding author: Aysun Sagbas
email: asagbas@nku.edu.tr

$$C_{pmk} = min\left(\frac{T_2 - \mu}{3 \cdot \sqrt{\sigma^2 + (\mu - T)^2}}, \frac{\mu - T_1}{3 \cdot \sqrt{\sigma^2 + (\mu - T)^2}}\right)$$

The C_p index considers the overall process variability relative to the manufacturing tolerance as a measure of process precision. The process capability ratio C_p does not take into account where the process mean is located relative to specifications. Kane (1986) introduced the index of C_{pk} to overcome this problem. The C_{pk} index is used to provide an indication of the variability of a process. It describes how well the process fits within the specification limits, taking into account the location of the process mean. Since the index C_{pk} provides a lower bound on the process yield, it has become the most popular capability index and is widely used in real-world applications. C_p and C_pk indices are not related to the cost of failing to meet customers' requirement of the target (Mahesh and Prabhuswamy, 2010; Tai, 2011; Jiao and Djurdjanovic, 2010; Chang and Wu, 2008). To take the target value into account, Chena*et al*. (2012) introduced the index of C_{pm}, which was also later, proposed independently by Chen *et al*. (2001). This index is motivated by the idea of squared error loss and this loss-based process capability index of C_{pm} is sometimes called as Taguchi index. The process capability index of C_{pm} is used to assess the ability of a process to be clustered around a target. The C_{pm} index incorporates two variation components which are variation to the process mean and deviation of the process mean from the target. Pearn*et al*. (1992) proposed the process capability index of C_{pmk}, which combines the features of the three earlier indices, namely C_p, C_{pk}, and C_{pm}. The C_{pmk} index alerts the user whenever the process variance increases and the process mean deviates from its target value. Process capability indices are not only used for measuring the manufacturing yield but also used for evaluation of the performance of outsourcing suppliers. Therefore, an accurate evaluation of the process capability is very essential in supply chain management. In manufacturing processes, some inevitable process fluctuations may be undetected when the statistical process control charts are applied (Perakis, 2010). Many authors (Pearnand Shu, 2003; Wu *et al*., 2009; Jeang, 2010; Chena *et al*., 2012; Grau, 2011; Lin, 2006; Hsu *et al*., 2007; Bordignon and Scagliarini, 2006) have promoted the use of various PCIs and examined them with a different degree of completeness. Boyles (1991) conducted an approximate method for finding lower confidence limits of C_{pm}. Pearn *et al*. (2005) provided a mathematical derivation of upper bound formula for C_{pmk} on process yield, in terms of the number of nonconformities. Existing research works have reported the capability modifications which only cover either undetected mean shift or undetected variance change. The idea of using one chart for monitoring process mean and variance was considered by Chan *et al*. (1988). Costa and Rahim (2004) proposed a single chart based on the non-central Chi-Square statistic for monitoring both the process mean and variance. Pearn *et al*. (2004) and Chen *et al*. (2001) considered extensions of C_{pm} and C_{pmk} to handle a process with asymmetric tolerances. They derived the explicit forms of the probability density function and the cumulative density function of the estimator of C_{pm} and C_{pmk} under the assumption of normal distribution. The traditional approach for monitoring a process subject to shifts in the mean and an increase in the variance is to use joint $\bar{X}$ and R charts. In this paper, we have proposed a new process capability chart, a single chart, for the surveillance of both the process mean and the variance. These charts are not only detectingjoints the variations in the mean and the standard deviation of the process, but also control the proportion of nonconforming items, that

show the deviation of the process from specification limits. Also, proposed approach is simple to understand whether a given process meets the capability requirements. The main goal of this study is to investigate the efficiency of the capability C_{pm} and C_{pmk} control charts. To calculate the efficiency and the control limits of the proposed charts, a new approach is developed using some distributions such as non-central Chi-Square, ω and φ distributions. In addition, the proposed capability control charts are compared with a joint $\bar{X}$ and R charts.

2. Distribution of the Estimated C_{pm}

The Taguchi capability index of C_{pm} is based on a measure of the process variation from target value and is therefore sensitive to process centering as well as process yield. Since C_{pm} simultaneously measures process variability and centering, a C_{pm} control chart would provide a convenient way to monitor changes in process capability after statistical control is established

Let $x_1, x_2,...x_n$ denote a random sample of n measurements on the process characteristic of interest, assumed to be normally distributed. Let $\bar{x}$ and s_{n-1} denote the usual estimated mean and the standard deviation for observation subgroups. Boyles (1991) and Chan *et al.* (1988) proposed the following estimator of C_{pm}:

$$\widehat{C}_{pm} = \frac{T_2 - T_1}{6 \cdot \sqrt{\frac{n-1}{n} \cdot s_{n-1}^2 + (\bar{x} - T)^2}} = \frac{T_2 - T_1}{6 \cdot \sqrt{s_n^2 + (\bar{x} - T)^2}} \quad (2)$$

Where; $\bar{x}$ and s_n^2 are the estimator of μ and σ^2, respectively.

In this study, the estimation of the cumulative distribution function of C_{pm} is derived using ω distribution and Chi-Square distribution.

2.1 Estimation of C_{pm} using ω distribution

Using Equation (2) we can transform the estimator of C_{pm} as below:

$$\hat{C}_{pm} = \frac{T_2 - T_1}{6 \cdot \sqrt{s_n^2 + (\bar{x} - T)^2}} = \frac{\frac{T_2 - T_1}{2} \frac{\sqrt{n}}{\sigma}}{3 \cdot \frac{\sqrt{n}}{\sigma} \cdot \sqrt{s_n^2 + (\bar{x} - T)^2}} = \frac{\frac{T_2 - T_1}{2} \frac{\sqrt{n}}{\sigma}}{3 \cdot \sqrt{n \frac{s_n^2}{\sigma^2} + n \left(\frac{\bar{x} - T}{\sigma}\right)^2}}$$

Changing variable with $D = \frac{T_2 - T_1}{2}$ and $d = D \cdot \frac{\sqrt{n}}{\sigma}$, we obtain Equation (3).

$$\hat{C}_{pm} \sim \frac{D \cdot \frac{\sqrt{n}}{\sigma}}{3 \cdot \sqrt{\frac{\chi_{n-1}^2 + N\left(\sqrt{n} \cdot \frac{\mu - T}{\sigma}, 1\right)^2}{}}} = \frac{d}{3 \cdot \sqrt{\chi_{n-1}^2 + Y}} \quad (3)$$

Where D is semi-width interval, d is a standardized value of the interval midpoint, and Y is a squared normal distributed with mean $\sqrt{n} \cdot \frac{\mu - T}{\sigma}$ and standard deviation of 1.

Based on Equation (3), we can obtain the cumulative distribution function (CDF) of $\hat{C}_{pm}$ using ω distribution. It is expressed in Equation (4).

$$F_{\hat{C}_{pm}}(\omega) = P\left(\hat{C}_{pm} \leq \omega\right) = P\left(\frac{d}{3 \cdot \sqrt{\chi_{n-1}^2 + Y}} \leq \omega\right) = P\left(\left(\frac{d}{\omega \cdot 3}\right)^2 - Y \leq \chi_{n-1}^2\right) \quad (4)$$

Where ω denotes $\hat{C}_{pm}$ random variable and takes only positives values.

Using Equation (4), we can compute the CDF of $\widehat{C}_{pm}$ as follows:

$$F_{\hat{C}_{pm}}(\omega) = P\left(\chi^2_{n-1} \geq \left(\frac{d}{\omega \cdot 3}\right)^2 - Y\right) = \int_0^{\left(\frac{d}{\omega \cdot 3}\right)^2} \int_{\left(\frac{d}{\omega \cdot 3}\right)^2 - Y}^{\infty} \frac{f_Z(-\sqrt{Y}) + f_Z(\sqrt{Y})}{2 \cdot \sqrt{Y}} \cdot f_{\chi^2_{n-1}}(\chi^2_{n-1}) \cdot d\chi^2_{n-1} \cdot dY = 1 - 0 d\omega \cdot 32 f Z - Y + f Z Y 2 \cdot Y \cdot F \chi n - 12 d\omega \cdot 32 - Y \cdot dY \quad (5)$$

Where $f_z(\cdot)$ is the density function of a normal distribution with mean $\sqrt{n} \cdot \frac{\mu - T}{\sigma}$ and standard deviation of 1.

Cumulative distribution function of $\hat{C}_{pm}$ using ω distribution is given in Figure 1.

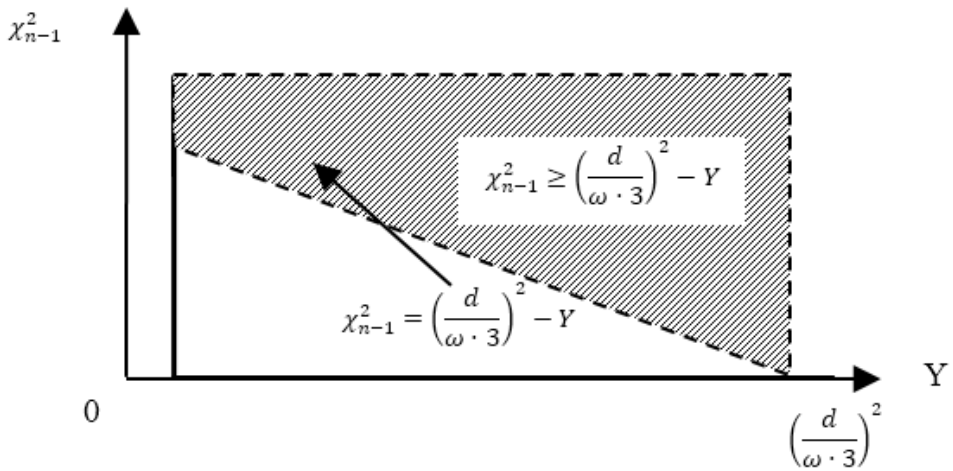

Figure 1. Cumulative distribution function of $\hat{C}_{pm}$ using ω distribution

The estimated capability index, $\hat{C}_{pm}$ is a random variable with *ω* distribution. So, the cumulative distribution function of $\hat{C}_{pm}$ can be used to calculate the control chart limits and efficiency of the control chart.

2.2 Estimation of C_{pm} using chi-square distribution

Using the representation in Equation 2, $\hat{C}_{pm}$ can be rewrittenas below:

$$\hat{C}_{pm} = \frac{T_2 - T_1}{6 \cdot \sqrt{s_n^2 + (\bar{x} - T)^2}} = \frac{T_2 - T_1}{6 \cdot \frac{\sigma}{\sqrt{n}} \cdot \sqrt{\frac{n}{\sigma^2} s_n^2 + n \cdot \left(\frac{\bar{x} - T}{\sigma}\right)^2}}$$

To derive the probability density function and the cumulative distribution function of $\hat{C}_{pm}$ the estimator of C_{pm} can be expressed as:

$$\hat{C}_{pm} = \frac{T_2 - T_1}{6 \cdot \frac{\sigma}{\sqrt{n}} \sqrt{\frac{n \cdot s_n^2}{\sigma^2} + n \cdot \left(\frac{\bar{x} - T}{\sigma}\right)^2}} \equiv \frac{T_2 - T_1}{6 \cdot \frac{\sigma}{\sqrt{n}} \sqrt{\chi^2_{n,\lambda}}} = \frac{d}{3\sqrt{\chi^2_{n,\lambda}}} \quad (6)$$

Where $\chi^2_{n,\lambda}$ denotes a non-central Chi-Square distribution with n degrees of freedom and we get:

$$\lambda = n \cdot \left(\frac{\mu - T}{\sigma}\right)^2$$

Where λ is the parameter of the non-central Chi-Square distribution.

3. Control chart limits for C_{pm}

Specifying the control limit is one of the critical decisions that must be made in designing a control chart. These control limits are chosen so that if the process is in control, all of the sample points will fall between them. As long as the points plot within the control limits, the process is assumed to be in control, and no action is necessary. However, a point that plots outside of the control limits is interpreted as evidence that the process is out of control, and investigation and corrective action is required to find and eliminate the assignable cause (Lin and Sheen, 2005; Maiko *et al.*, 2009). Essentially, the control chart is a test of the hypothesis that the process is in a state of statistical control. To determine if a given process meets the preset capability requirement, we can consider the statistical testing with null hypothesis H_0 ($C_{pm} = C_{pm0}$) and alternative hypothesis H_1 ($C_{pm} \neq C_{pm0}$). For an initial study, we use the samples that are in control to calculate the value of C_{pm0}using the estimators $\hat{\mu}=\bar{\bar{x}}$ for process mean and $\hat{\sigma} = \bar{s}_n/c_2$ for standard deviation.

$$P\left(a \leq \hat{C}_{pm} \leq b \middle| C_{pm} = C_{pm\,0}\right) = 1 - \alpha$$

Where a denotes lower confidence limit and b denotes upper confidence limit, C_{pm0} denotes Taguchi capability index when the process is in control.

Considering Equation (7), we obtain the distribution of $\hat{C}_{pm}$ given in Figure 2. The distribution of $\hat{C}_{pm}$ is constructed using Mathcad software.

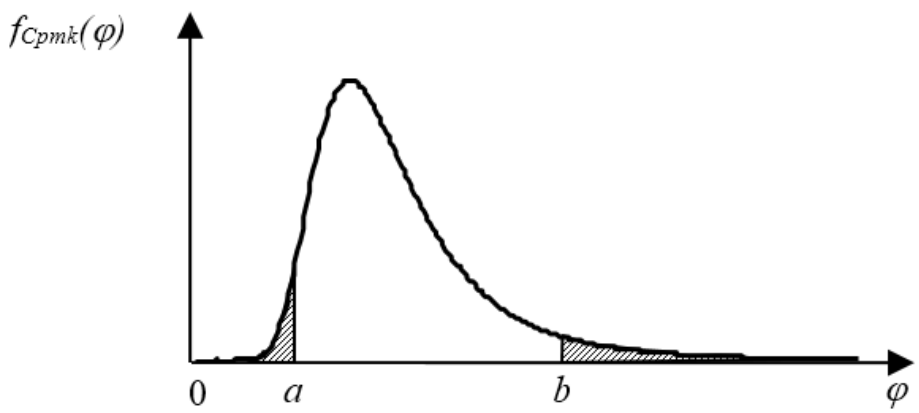

Figure 2. Distribution of the estimated C_{pm}

3.1 Calculation of control limits using ω distribution

Numerous methods for constructing approximate confidence interval have been proposed in the literature (Costa, 1998; Novoa and Noel, 2008). In this paper, the control graphic limits are computed using ω distribution and Chi-Square distribution. Firstly, the control limits using ω distribution is constructed. A 100 (1 - α) % confidence interval estimation is shown in Equation (8).

$$P\left(a \leq \hat{C}_{pm} \leq b/C_{pm} = C_{pm\,0}\right) = 1 - \alpha \quad (8)$$

Using the distribution function of ω the control limits are computes as:

$$a = \omega_0^{1-\alpha/2} \text{and} b = \omega_0^{\alpha/2}$$

And upper and lower control limits of C_{pm} can be expressed as below:

$$UCL_{Cpm} = \omega_0^{\alpha/2}$$

$$CL_{Cpm} = C_{pm\,0}$$

$$LCL_{Cpm} = \omega_0^{1-\alpha/2}$$

3.2 Calculation of control limits using Chi-Square distribution

We can also compute the control limits using Chi-Square distribution. Replacing the estimator of *Cpm* in the Chi-Square distribution, we can obtain a 100(1-α)% confidence interval estimation shown in Equation (9).

$$P\left(a \le \frac{d_0}{3\sqrt{\chi^2_{n,\lambda_0}}} \le b\right) = 1 - \alpha \qquad (9)$$

Hence, we get

$$P\left(\frac{3a}{d_0} \le \frac{1}{\sqrt{\chi^2_{n,\lambda_0}}} \le \frac{3b}{d_0}\right) = 1 - \alpha$$

By some simplifications:

$$P\left(\frac{d_0^2}{9a^2} \ge \chi^2_{n,\lambda_0} \ge \frac{d_0^2}{9b^2}\right) = 1 - \alpha$$

Using the Chi-Square distribution, the control limits are computed as follows:

$$a = \frac{d_0}{3\cdot\sqrt{\chi^{2(\alpha/2)}_{n,\lambda_0}}} \text{and} b = \frac{d_0}{3\cdot\sqrt{\chi^{2(1-\alpha/2)}_{n,\lambda_0}}}$$

And upper control limit and lower control limit can be expressed as:

$$UCL_{Cpm} = \frac{d_0}{3\cdot\sqrt{\chi^{2(1-\alpha/2)}_{n,\lambda_0}}}$$

$$CL_{Cpm} = C_{pm\,0}$$

$$LCL_{Cpm} = \frac{d_0}{3\cdot\sqrt{\chi^{2(\alpha/2)}_{n,\lambda_0}}}$$

3.3 Efficiency study on C_{pm} using ω distribution

The efficiency of control chart is determined by average run length. The speed with which a control chart detects process shift measures its statistical efficiency. An efficient chart balances the cost by operating out-of-control and the cost of maintaining the control chart. However, for fixed chart costs, the quicker and out-of-control state is detected, the better is the quality of a chart. The ability of control charts to detect shifts in process is described by their operating characteristic curves. The operating characteristics of $\hat{C}_{pm}$ can be defined as:

$$Pa = P\left(LCL_{Cpm} \le \hat{C}_{pm} \le UCL_{Cpm}/C_{pm}\right)$$

Replacing the value of control limits defined in previous section, we have:

$$Pa = P\left(\omega_0^{1-\alpha/2} \le \hat{C}_{pm} \le \omega_0^{\alpha/2}/C_{pm}\right)$$

Where ω_0 is the value of C_{pm} for $\mu_0$and σ_0. Using cumulative distribution function, the operating characteristics take the form below:

$$Pa = F_{\hat{C}_{pm}}\left(\omega_0^{\alpha/2}\right) - F_{\hat{C}_{pm}}\left(\omega_0^{1-\alpha/2}\right) \qquad (10)$$

3.4 Efficiency study on C_{pm} using Chi-square distribution

The operating characteristics provide a measure of the efficiency of the control charts. They display the probability of incorrectly accepting the hypothesis of statistical control.Using the value of control limits computed in previous section, the operating characteristic of $\hat{C}_{pm}$ can be established as:

$$Pa = P\left(LCL_{Cpm} \le \hat{C}_{pm} \le UCL_{Cpm}/C_{pm}\right) = P\left(\frac{d_0}{3\cdot\sqrt{\chi^{2(\alpha/2)}_{n,\lambda_0}}} \le \hat{C}_{pm} \le \frac{d_0}{3\cdot\sqrt{\chi^{2(1-\alpha/2)}_{n,\lambda_0}}}\right)$$

By some simplifications, we can construct the operating characteristics as below:

$$Pa = P\left(\frac{T_2 - T_1}{6\cdot\frac{\sigma_0}{\sqrt{n}}\cdot\sqrt{\chi^{2(\alpha/2)}_{n,\lambda_0}}} \le \frac{T_2 - T_1}{6\cdot\frac{\sigma}{\sqrt{n}}\cdot\sqrt{\chi^{2(\alpha/2)}_{n,\lambda_0}}} \le \frac{T_2 - T_1}{6\cdot\frac{\sigma_0}{\sqrt{n}}\cdot\sqrt{\chi^{2(1-\alpha/2)}_{n,\lambda_0}}}\right)$$

And we have:

$$Pa = \left(\frac{\sigma_0^2}{\sigma^2}\cdot\chi^{2\left(\frac{\alpha}{2}\right)}_{n,\lambda_0} \ge \chi^2_{n,\lambda} \ge \frac{\sigma_0^2}{\sigma^2}\cdot\chi^{2\left(1-\frac{\alpha}{2}\right)}_{n,\lambda_0}\right) = \left(\frac{\chi^{2(\alpha/2)}_{n,\lambda_0}}{r_v} \ge \chi^2_{n,\lambda} \ge \frac{\chi^{2(1-\alpha/2)}_{n,\lambda_0}}{r_v}\right)$$

$$Pa(r_{Cpm}) = F_{\chi^2_{n,\lambda}}\left(\frac{\chi^{2(\alpha/2)}_{n,\lambda_0}}{r_v}\right) - F_{\chi^2_{n,\lambda}}\left(\frac{\chi^{2(1-\alpha/2)}_{n,\lambda_0}}{r_v}\right)$$

Where r_v is the variance ratio.

Also, using the cumulative distribution function of $\hat{C}_{pm}$, the operating characteristics can be written as:

Where the probability density function of a non-central Chi-Square with n degree of freedom is given in Equation (12).

$$f_{\chi^2_{n,\lambda}}(x) = e^{-\frac{\lambda}{2}}\cdot\sum_{i=0}^{\infty}\frac{\lambda^i}{i!}\cdot\frac{x^{\frac{n}{2}+i-1}\cdot e^{-\frac{x}{2}}}{2^{\frac{n}{2}+2i}\cdot\Gamma\left(\frac{n}{2}+i\right)}x > 0 \quad (12)$$

And the cumulative distribution function can be shown as below:

$$F_{\chi^2_{n,\lambda}}(x) = \int_0^x e^{-\frac{\lambda}{2}}\cdot\sum_{i=0}^{\infty}\frac{\lambda^i}{i!}\cdot\frac{y^{\frac{n}{2}+i-1}\cdot e^{-\frac{y}{2}}}{2^{\frac{n}{2}+2i}\cdot\Gamma\left(\frac{n}{2}+i\right)}\cdot dyx > 0 \quad (13)$$

4. Distribution of the Estimated C_{pmk}

The index of C_{pmk} takes into account the location of the process mean between two specification limits, the proximity to the target value, and the process variation. It has been shown to be a useful capability index for processes with two-sided specification limits. If the target value is centered in the tolerance interval midpoint (T=M), the C_{pmk} index can be defined as:

$$C_{pmk} = \frac{min\,(T_2-\mu,\mu-T_1)}{3\cdot\sqrt{\sigma^2+(\mu-T)^2}}$$

We know that:

$$min(x,y) = \frac{1}{2}\cdot(x+y) - \frac{1}{2}\cdot|x-y|$$

And then, we can write C_{pmk} as:

$$C_{pmk} = \frac{\frac{T_2-T_1}{2} - \left|\frac{T_2+T_1}{2} - \mu\right|}{3\cdot\sqrt{\sigma^2+(\mu-T)^2}} = \frac{D-|M-\mu|}{3\cdot\sqrt{\sigma^2+(\mu-T)^2}} = \frac{D-|\mu-T|}{3\cdot\sqrt{\sigma^2+(\mu-T)^2}}$$

Using above Equation, we can express the estimator of C_{pmk}:

Changing some variables, $\hat{C}_{pmk}$ distribution is written as:

$$\hat{C}_{pmk} = \frac{D-|\bar{x}-T|}{3\cdot\sqrt{s_n^2+(\bar{x}-T)^2}} \qquad (14)$$

$$\hat{C}_{pmk} = \sim \frac{D-\left|\sqrt{N\left(\mu,\frac{\sigma}{\sqrt{n}}\right)^2}-T\right|}{\frac{3\sigma}{\sqrt{n}}\cdot\sqrt{\chi^2_{n-1}+\mathrm{n}\cdot\mathrm{N}\left(\frac{\mu-\mathrm{T}}{\sigma},\frac{1}{\sqrt{\mathrm{n}}}\right)^2}} = \frac{\frac{D\cdot\sqrt{n}}{\sigma}-\left|\sqrt{N\left(\frac{\mu-T}{\sigma}\sqrt{n},1\right)^2}\right|}{3\cdot\sqrt{\chi^2_{n-1}+\mathrm{N}\left(\frac{\mu-\mathrm{T}}{\sigma}\sqrt{n},1\right)^2}}$$

By some simplifications, we have:

$$\hat{C}_{pmk} = \frac{d-|\sqrt{Y}|}{3\cdot\sqrt{\chi^2_{n-1}+Y}} \qquad (15)$$

cumulative distribution function of $\hat{C}_{pmk}$ using φ distribution, as expressed in Equation (16).

Based on Equation (15), we can obtain the

$$F_{\hat{C}_{pmk}}(\varphi) = P\left(\hat{C}_{pmk} \le \varphi\right) = P\left(\frac{d-|\sqrt{Y}|}{3\cdot\sqrt{\chi^2_{n-1}+Y}} \le \varphi\right) = P\left(\frac{d-|\sqrt{Y}|}{3\cdot\varphi} \le \sqrt{\chi^2_{n-1}+Y}\right)$$

$$P\left(\left(\frac{d-|\sqrt{Y}|}{3\cdot\varphi}\right)^2 \le \chi^2_{n-1}+Y\right) = P\left(\left(\frac{d-|\sqrt{Y}|}{3\cdot\varphi}\right)^2 - Y \le \chi^2_{n-1}\right) \qquad (16)$$

Where φ denotes $\hat{C}_{pmk}$andom variable and takes only positives values.

Cumulative distribution function of $\hat{C}_{pmk}$ defined in Equation (16) is given in Figure 3.

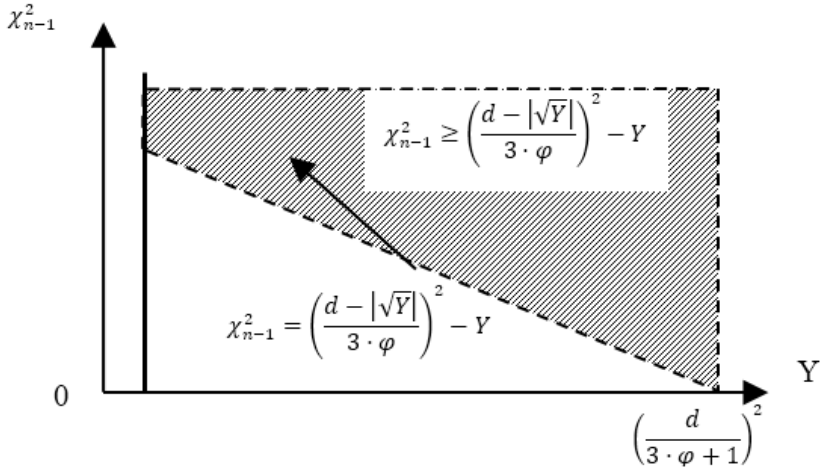

Figure 3. Cumulative distribution function of $\hat{C}_{pmk}$ using Chi-Square distribution

Using Equation (16), we can compute the cumulative distribution function of $\hat{C}_{pmk}$ as below:

$$F_{\hat{C}pmk} = P\left(\chi_n^2 \geq \left(\frac{d-|\sqrt{Y}|}{3\cdot\varphi}\right)^2 - Y\right) = \int_0^{\left(\frac{d}{3\cdot\varphi+1}\right)^2} \int_{\left(\frac{d-\sqrt{Y}}{3\cdot\varphi}\right)^2 - Y}^{\infty} \frac{f_Z(-|\sqrt{Y}|)+f_Z(|\sqrt{Y}|)}{2\cdot|\sqrt{Y}|} \cdot f_{\chi^2_{n-1}}(\chi^2_{n-1}) \cdot$$

$$d\chi n{-}12{\cdot}dY{=}1{-}0d3{\cdot}\varphi{+}12fZ{-}Y{+}fZY2{\cdot}Y{\cdot}F\chi n{-}12d{-}Y3{\cdot}\varphi2{-}dY \quad (17)$$

4.1 Control chart limits for C_{pmk}

To determine if a given process meets the preset capability requirement, we can consider the statistical testing with null hypothesis H_0 ($C_{pmk} = C_{pmk0}$) and alternative hypothesis H_1 ($C_{pmk} \neq C_{pmk0}$). In this study, we search two control limits, namely *a* and*b* computed below:

$$P\left(a \leq \hat{C}_{pmk} \leq b \mid C_{pmk} = C_{pmk\,0}\right) = 1 - \alpha$$

Where C_{pmk0} is Taguchi real capability index when the process is in control.

Considering above Equation, we obtain the distribution of $\hat{C}_{pmk}$ given in Figure 4. To construct the distribution of $\hat{C}_{pmk}$ is conducted Mathcad software.

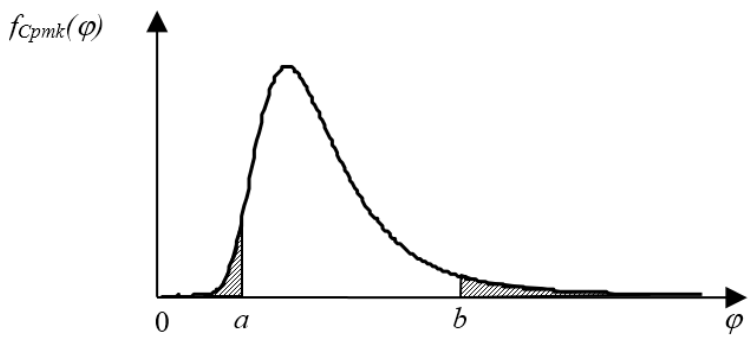

Figure 4. Distribution of the Estimated C_{pmk}

Using the distribution function of $\hat{C}_{pmk}$, the values of *a* and*b* are computed as:

$$a = \varphi_0^{1-\alpha/2} \text{and} b = \varphi_0^{\alpha/2}$$

And the control limits for *Cpmk* can be expressed as below:

$$UCL_{Cpmk} = \varphi_0^{\alpha/2}$$

$$CL_{Cpmk} = C_{pmk\,0}$$

$$LCL_{Cpmk} = \varphi_0^{1-\alpha/2}$$

Where UCL_{Cpmk} is the upper control limit of *Cpmk*, CL_{Cpmk} is the center line of *Cpmk* and LCL_{Cpmk} is the lower control limit of C_{pmk}.

4.2 Efficiency study on C_{pmk}

Process variation, process departure and process loss have been considered crucial benchmarks for measuring process performance. The ability of *Cpmk* control charts to detect shifts in process is described by their operating characteristic curves. The operating characteristics of $\hat{C}_{pmk}$ can be defined as:

$$Pa = P\left(LCL_{Cpmk} \leq \hat{C}_{pmk} \leq UCL_{Cpmk} \,|C_{pmk}\right)$$

Using the value of control limits computed in Section 4.1, the operating characteristic of $\hat{C}_{pmk}$ can be constructed as:

$$Pa = P\left(\varphi_0^{1-\alpha/2} \leq \hat{C}_{pmk} \leq \varphi_0^{\alpha/2}\right) = F_{\hat{C}_{pmk}}\left(\varphi_0^{\alpha/2}\right) - F_{\hat{C}_{pmk}}\left(\varphi_0^{1-\alpha/2}\right) \qquad (18)$$

Where φ_0 is the value of C_{pmk} for μ_0 and σ_0.

5. Efficiency comparison of the capability control charts with joint $\bar{X}$ and *R* charts

The purpose of the process monitoring is the detection of any assignable causes that changes μ from μ_0 to $\mu_1 = \mu_0 + \delta\sigma_0$, where $\delta \neq 0$ and that changes σ fromσ_0 to$\sigma_1 = \gamma\sigma_0$, where $\gamma \neq 0$. Varying the values of μ and σ, we obtain the efficiency of capability control charts and joint $\bar{X}$ and *R* control charts. For a control chart, the detection speed of the process shifts shows its statistical performance. In this section, the performance of C_{pm} and C_{pmk} capability control charts is compared with the performance of a traditional $\bar{X}$ and *R* control charts. We use as sample size values of *n*=3 and *n*=5, that are the most usual. The C_{pm} control chart has been obtained using the ω distribution of the C_{pm}, and the C_{pmk} controlchart has been obtained using the φ distribution of the C_{pmk}. The numerical examples given in Costa's paper (1998) are used to compare the results. The obtained results are displayed in Tables 1 and 2. Table 1 presents the efficiency values both capability-traditional control charts for sample size of 3.

As seen in Table 1, for given sample size of *n*, the performance of all the control charts increases as δ and γ increases. For small values of γ ($\gamma \leq 1.75$), the $\bar{X}$ and *R* charts are better for detecting small shifts, but for large values of γ ($\gamma \geq 2$), C_{pm} chart are slightly better for detecting larger shifts. In other words, C_{pm} control chart catches the shifts faster than the joint $\bar{X}$ and *R* charts for γ=3, and both of them have almost same performance for γ=2. When δ increases ($\delta \geq 0.5$), for low values of γ (γ<1.5), C_{pmk} control chart are better for detecting assignable causes than C_{pm}control chart, conversely, for high values of γ ($\gamma \geq 1.5$), the performance of the C_{pm} control chart is better than C_{pmk} control chart. Table 2 summarizes the efficiency values for capability and traditional control charts for sample size of 5.

From Table 2, it is evident that when δ and γ increases the performance of all the charts increases (except for the values of $\bar{X}$ and *R* charts, and C_{pmk} chart for $\delta = 2$). Also, when δ increases ($\delta \geq 0.5$) for especially large values of γ ($\gamma \geq 1.75$), C_{pm} control chart is the best for detecting assignable causes. For small values of γ ($\gamma \leq 1.5$), C_{pmk} control chart catches the shifts faster than C_{pm} control chart. After all, it is seen that, the results obtained for different sample size are similar.To compare the efficiency of C_{pm} and C_{pmk} control charts we provide the operating characteristics curves shown in Figure 5-8. For calculating the operating characteristics, we use the process parameters as *T*=5, T_1=4, T_2=6, μ_0=5, σ_0=0.2, *n*=5, $\alpha \approx 0.0024$. Figure 5 presents the operating characteristic curves of C_{pm} and C_{pmk} control charts (standard deviation is in control, process mean changes).

Table 1. The efficiency comparison of the control charts for n=3, with α=0.0024

n=3	δ=0			δ=0.5			δ=0.75		
	C_{pm}	C_{pmk}	$\bar{x}, R$	C_{pm}	C_{pmk}	$\bar{x}, R$	C_{pm}	C_{pmk}	$\bar{x}, R$
γ=1	0.998	0.998	0.998	0.995	0.991	0.990	0.988	0.976	0.973
γ=1.25	0.982	0.986	0.978	0.968	0.965	0.959	0.946	0.932	0.929
γ=1.5	0.930	0.95	0.923	0.904	0.916	0.896	0.871	0.872	0.859
γ=1.75	0.841	0.887	0.837	0.812	0.849	0.808	0.776	0.803	0.771
γ =2	0.735	0.804	0.735	0.708	0.769	0.708	0.676	0.727	0.676
γ =3	0.377	0.469	0.387	0.367	0.455	0.375	0.354	0.437	0.363
n=3	δ=1			δ=1.5			δ=2		
	C_{pm}	C_{pmk}	$\bar{x}, R$	C_{pm}	C_{pmk}	$\bar{x}, R$	C_{pm}	C_{pmk}	$\bar{x}, R$
γ=1	0.969	0.94	0.934	0.859	0.761	0.742	0.598	0.443	0.415
γ=1.25	0.907	0.876	0.876	0.763	0.687	0.690	0.530	0.425	0.425
γ=1.5	0.822	0.808	0.804	0.672	0.627	0.636	0.473	0.407	0.422
γ=1.75	0.726	0.740	0.719	0.590	0.576	0.576	0.424	0.39	0.405
γ =2	0.631	0.671	0.632	0.515	0.529	0.515	0.38	0.373	0.375
γ =3	0.337	0.414	0.346	0.291	0.353	0.301	0.238	0.283	0.248

Table 2. The Efficiency comparison of the control charts for n=5, with α=0.0024

n=5	δ=0			δ=0.5			δ=0.75		
	C_{pm}	C_{pmk}	$\bar{x}, R$	C_{pm}	C_{pmk}	$\bar{x}, R$	C_{pm}	C_{pmk}	$\bar{x}, R$
γ=1	0.998	0.998	0.998	0.997	0.986	0.982	0.982	0.953	0.941
γ=1.25	0.975	0.981	0.973	0.97	0.940	0.938	0.913	0.876	0.880
γ=1.5	0.888	0.920	0.894	0.878	0.857	0.849	0.791	0.777	0.786
γ=1.75	0.745	0.809	0.767	0.734	0.744	0.722	0.646	0.668	0.666
γ =2	0.587	0.672	0.621	0.578	0.618	0.585	0.506	0.556	0.539
γ =3	0.184	0.247	0.213	0.182	0.234	0.206	0.165	0.218	0.194
n=5	δ=1			δ=1.5			δ=2		
	C_{pm}	C_{pmk}	$\bar{x}, R$	C_{pm}	C_{pmk}	$\bar{x}, R$	C_{pm}	C_{pmk}	$\bar{x}, R$
γ=1	0.948	0.874	0.844	0.729	0.528	0.459	0.33	0.155	0.115
γ=1.25	0.845	0.770	0.777	0.600	0.459	0.459	0.289	0.169	0.160
γ=1.5	0.710	0.668	0.692	0.487	0.402	0.435	0.250	0.172	0.194
γ=1.75	0.573	0.571	0.588	0.392	0.352	0.390	0.214	0.168	0.200
γ =2	0.448	0.478	0.479	0.312	0.306	0.333	0.181	0.160	0.187
γ =3	0.151	0.198	0.180	0.118	0.150	0.138	0.083	0.101	0.099

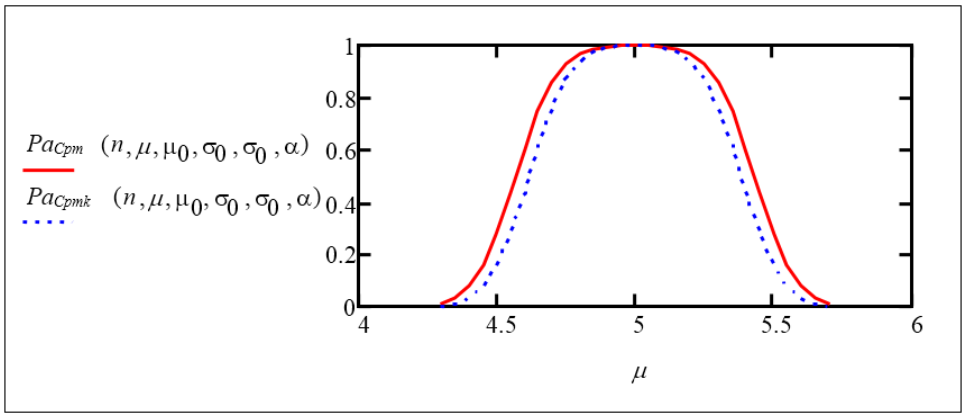

Figure 5. Operating characteristic curves of C_{pm} and C_{pmk} control charts ($\sigma=\sigma 0$)

We observe that C_{pmk} control chart has more power than C_{pm} control chart to detect the changes in the mean, assuming that standard deviation is constant. The operating characteristic curves of C_{pm} andC_{pmk} control charts are shown in Figure 6 (σ=0.5, process mean changes).

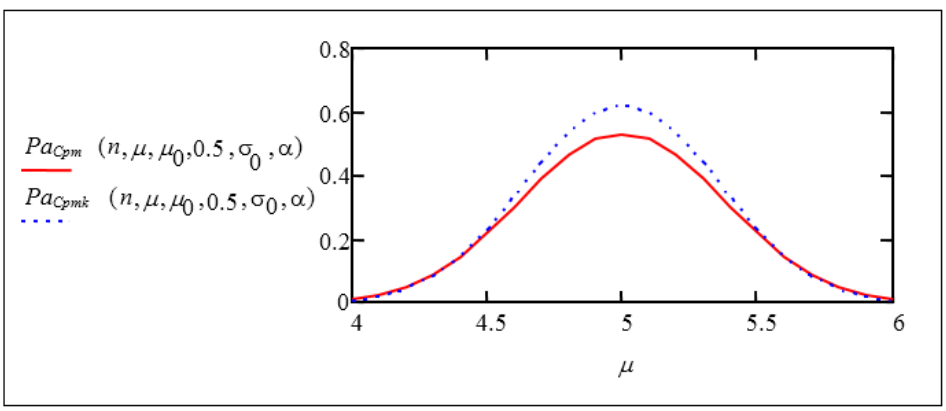

Figure 6. Operating characteristic curves of C_{pm} and C_{pmk} control charts (σ=0.5)

As seen in Figure 6, for a small changes in the process mean, the efficiency of the C_{pm} control chart is better than the C_{pmk}. Also, the performance of C_{pm} and C_{pmk} are almost same for larger shifts in the process mean.Figure 7 provides the operating characteristic curves of C_{pm} and C_{pmk} control charts (process mean is in control, standard deviation changes).

It is clear that both of the operating characteristic curves are very similar for all the values of the standard deviation. So, we ensure that, the performance of C_{pm} andC_{pmk} control charts is the same. Operating characteristics curves of C_{pm} and C_{pmk} control charts are given in Figure 8 (μ=5.6, process standard deviation changes). As seen in Figure 8, C_{pmk} control chart is more effective than C_{pm} control chart. It is concluded that, the performance of the C_{pm} control chart seems better for detecting changes in the process mean. However, C_{pmk} control chart is better for detecting changes in the process variance.

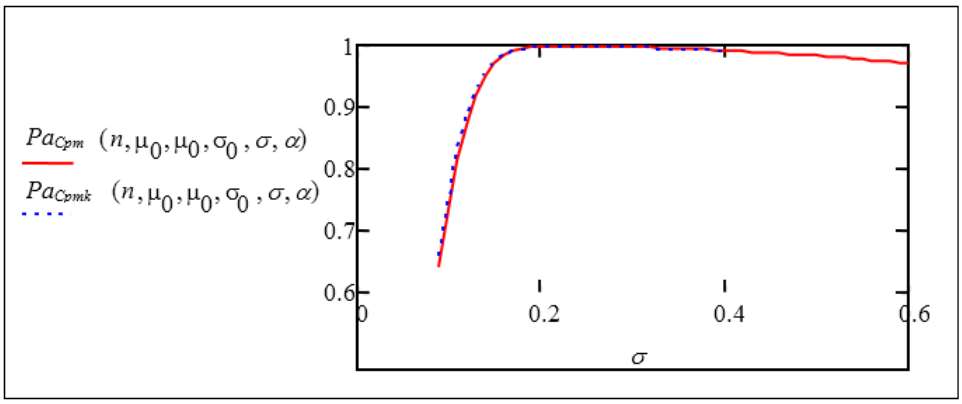

Figure 7. Operating characteristic curves of C_{pm} and C_{pmk} control charts (μ=μ_0)

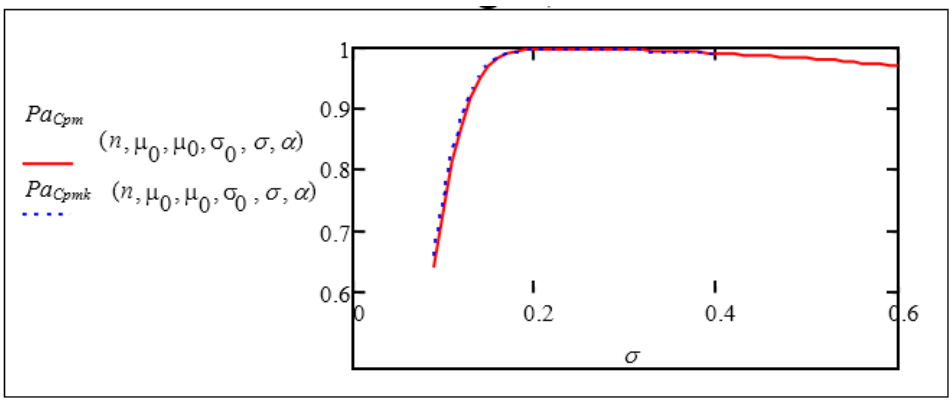

Figure 8. Operating characteristic curves of C_{pm} and C_{pmk} control charts (μ=5.6)

6. Application example: a simulation study

We consider an example to illustrate the design procedure which is described in the previous section. In order to test the applicability of the proposed C_{pm} control chart we conduct a simulation study. In this study, a random sample size of 5, for 25 subgroups was generated by simulation. The obtained results are displayed in Table 3.

Under the assumption that, these samples are taken from the normal distribution with mean 5 and standard deviation of 0.2. Using the ω distribution which is previously explained, we obtain the upper control limit *UCL*, is set to 7.827, the lower control limit, *LCL*, is set to 0.8349. The control chart of C_{pm} for the generated sample data is shown in Figure 9.

Table 3. Generated sample data

Sample	Data					$\bar{X}$	s_n^2	C_{pm}
1	4.912	4.864	4.905	4.81	4.663	4.8308	0.0084	1.7329
2	5.009	4.976	5.111	5.438	5.162	5.1392	0.0269	1.5496
3	5.197	5.172	5.183	5.135	4.791	5.0957	0.0236	1.8415
4	5.014	4.849	5.139	4.964	4.871	4.9674	0.0110	3.0334
5	4.855	4.897	5.112	4.951	5.018	4.9665	0.0082	3.4469
6	5.252	4.859	5.000	5.222	5.179	5.1023	0.0224	1.8375
7	4.42	4.569	5.041	4.877	4.76	4.7334	0.0483	0.9647
8	5.02	5.154	5.061	5.002	4.847	5.0169	0.0099	3.2915
9	4.918	4.865	4.974	5.204	5.036	4.9993	0.0137	2.8515
10	5.103	5.148	4.997	5.056	5.032	5.0671	0.0028	3.8960
11	5.086	4.905	4.861	5.61	4.943	5.0808	0.0756	1.1631
12	4.744	5.152	4.921	4.759	4.793	4.8739	0.0232	1.6848
13	4.996	5.006	5.053	5.098	5.048	5.0403	0.0013	6.1270
14	4.863	4.677	5.282	5.194	4.769	4.9571	0.0569	1.3748
15	5.029	5.339	4.936	4.594	4.718	4.9231	0.0671	1.2340
16	4.735	4.897	5.012	4.881	4.934	4.8917	0.0082	2.3608
17	5.108	5.044	5.081	4.769	4.779	4.9561	0.0226	2.1304
18	4.779	4.919	4.737	4.432	5.255	4.8245	0.0716	1.0415
19	5.158	5.029	4.799	4.815	4.824	4.9249	0.0207	2.0549
20	5.056	4.92	5.26	4.724	5.076	5.0072	0.0318	1.8686
21	5.088	5.352	4.871	5.11	5.309	5.1459	0.0299	1.4726
22	4.636	5.262	4.79	5.092	4.79	4.9138	0.0521	1.3656
23	4.752	5.085	4.617	4.975	5.083	4.9022	0.0351	1.5774
24	5.293	4.754	4.923	5.095	5.037	5.0206	0.0321	1.8478
25	5.039	5.104	5.165	5.186	5.179	5.1347	0.0031	2.2854

Summary statistics: $\hat{\mu} = \bar{\bar{x}} = 4.9806$; $\hat{\sigma}^2 = 0.0393$; $\hat{C}_{pm} = 1.67$

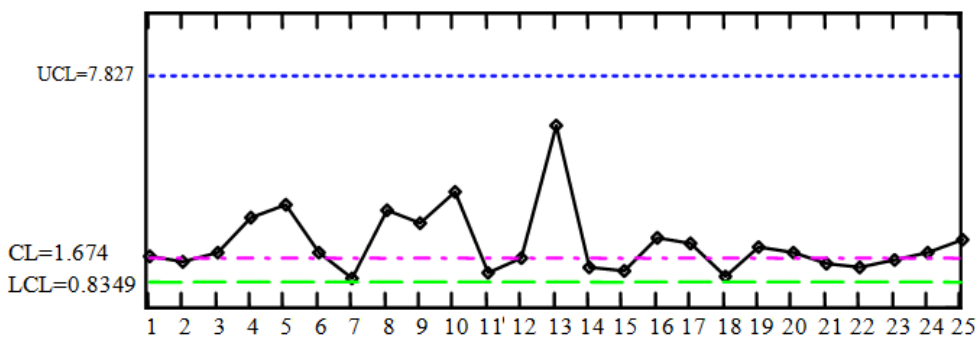

Figure 9. The Control chart of C_{pm} for the generated sample data

Using C_{pm} control chart, we conclude that process seems to be capable for initial study. We can recommend using C_{pm} for determining whether products meet

specifications. It is seen that the proposed approach can be applied in a simple way. To control the process using the C_{pmk} control chart, the procedure is similar. To derive C_{pmk} control chart same calculations can be performed the over the same observations.

7. Conclusions

Traditionally, and $\bar{X}$ chart is used to control the process mean and aR chart is used to control the process variance. In this paper, we propose a new process capability control chart design for monitoring the process mean, standart deviation simultaneously. Since capability control chartssimultaneously measures process variability and centering they would provide a convenient way to monitor changes in process capability after statistical control is established. We have shown that it is possible to design one chart which can monitor the mean, variability and the deviation from the specification limits at the same time.In this study, the efficiency of C_{pm} and C_{pmk} capability control charts are investigated. In addition, the efficiency of the proposed C_{pm} and C_{pmk} control charts is compared with a joint $\bar{X}$ and R control charts. It is seen that C_{pm} control chart is more effective to detect the changes in the process mean. Nevertheless, C_{pmk} control chart has more power to detect the changes in the process variance.It is demonstrated that how the new developed approach efficiently monitors capable but unstable processes by detecting the variation of the capability level. When the process shift is large the practitioners can use the suggested capability control chart design efficiently. The designed capability control charts are very useful in the case where one wants to compare the efficiency of the capability and traditional joint $\bar{X}$-R control charts, since, none of the techniques proposed in the literature, so far, can be used in such cases.

References:

Bordignon, S., & Scagliarini, M. (2006). Estimation of Cpmwhen measurement error is present. *Quality and Reliability Engineering International*. *22*(7), 787–801.

Boyles, R.A. (1991). The Taguchi capability index. *Journal of Quality Technology*, *23*(1), 17-26.

Chan, L.K., Cheng, S.W., & Spiring, F.A. (1988). A new measure of process capability: Cpm. *Journal of Quality Technology*, *29*(3),162-165.

Chang, Y. C., & Wu, C.W. (2008). Assessing process capability based on the lower confidence

Chen, G., Cheng, S.W., & Xie, H. (2001). Monitoring process mean and variability with one EWMA chart. *Journal of Quality Technology*, *33*, 223–233.

Chena, J., Zhubc, F., Lib, G.Y., Maa, Y.Z., & Tuc, Y.L. (2012). Capability index of a complex-product machining process. *International Journal of Production Research*, *50*(12), 3382–3394.

Costa, A.F. (1998). Joint $\overline{X}$ and R charts with variable parameters. *IIE Transactions. 30*, 505-514.

Costa, A.F., & Rahim, M.A. (2004). Monitoring process mean and variability with one non-central Chi-Square chart. *Journal of Applied Statistics*, *31*(10), 1171–1183.

Grau, D. (2011). Process yield and capability indices, Communications in Statistics—Theory and Methods, 40, 2751–2771.

Hsu, M., Shu, M.H., & Pearn, W.L. (2007). Measuring process capability based on Cpmk with gauge measurement errors. *Quality and Reliability Engineering International*. 23,597–614.

Jeang, A. (2010). Optimal process capability analysis for process design. *International Journal of Production Research*. *48*(4), 957–989

Jiao, Y.B., & Djurdjanovic, D. (2010). Joint allocation of measurement points and controllable tooling machines in multistage manufacturing processes. *IIE Transactions*, *42*(10), 703–720.

Kane, V.E. (1986). Process capability indices. *Journal of Quality Technology*. *18*(1), 41-52.

Lin, G.H. (2006). Evaluating process centering with large samples – an approximate lower bound on the accuracy index. *International Journal of Advanced Manufacturing Technology*. *28*, 149–153.

Lin, H.C., & Sheen, G.J. (2005). Practical implementation of the capability index Cpk based on the control chart data. *Quality Engineering*. *17*, 371-390.

Mahesh, B.P., & Prabhuswamy, M.S. (2010). Process variability reduction through statistical process control for quality improvement. *International Journal for Quality Research*. *4*(3), 193-203.

Maiko, M., Arizono, I., Nakase, I., & Takemoto, Y. (2009). Economical operation of the Cpm control chart for monitoring process capability index. I*nternational Journal of Advanced Manufacturing Technology*. *43*,304-311.

Novoa, C., & Noel, A.L. (2008). On the distribution of the usual estimator of Cpkand some applications in SPC. *Quality Engineering*, *21*, 24-32.

Pearn, W.L. Kotz, S., & Johnson, N.L. (1992). Distributional and inferential properties of process capability indices. *Journal of Quality Technology*, *24*(4), 216-231.

Pearn, W.L., & Lin, P.C. (2004). Testing process performance based on capability indices Cpk with critical values. *Computers and Industrial Engineering*, *47*, 351-369.

Pearn, W.L., & Shu, M.H. (2003). Lower confidence bounds with sample size information for Cpmapplied to production yield assurance. *International Journal of Production Research*. *41*(15), 581-3599.

Pearn, W.L., Shu, M.H., & Hsu, B.M. (2005). Testing process capability based on Cpm in the presence of random measurement errors. *Journal of Applied Statistics*, *32*(10), 1003-1024.

Perakis, M.(2010). Estimation of differences between process capability indices Cpm or Cpmk for two processes. *Journal of Statistical Computations and Simulation*. *80*(3),315-334.

Tai, Y.T. (2011). *Evaluating process capability under undetected fluctuations*. IEEE Int'l Technology Management Conference. 484-487.

Wu, C.W., Pearn, W.L., & Kotz, S. (2009). An overview of theory and practice on process capability indices for quality assurance. *International Journal Production Economics*. *117*, 338-359.

Appendix: Symbols used in the calculus:

n - sample size
$\bar{x}$ - samplemean
s_n - sample standard deviation
μ_0 - mean value when the process is in control
σ_0 - standard deviation when the process is in control
μ_1 - mean value when the process is out of control
σ_1 - standard deviation when the process is out of control
T - target value of the characteristic

T_1 - lower specification limit
T_2 - upper specification limit
M - tolerance interval midpoint
D - semi-width interval
λ - parameter of the non-central Chi-Square distribution
d - standardized value of the interval midpoint
C_{pm} - Taguchi capability index
C_{pm0} - Taguchi capability index whenwhen the process in control
C_{pmk} - Taguchi real capability index
C_{pmk0} - Taguchi real capability indexwhen the process in control
r_v - the variance ratio
ω - C_{pm} random variable
φ - C_{pmk} random variable
UCL - upper control limit
CL - central control line
LCL - lower control limit

María Teresa Carot
University of Valencia
Polytechnic,
Departament of Statistics
Operation Research and
Applied Quality
Valencia
Spain

Aysun Sagbas
University of Namik
Kemal
Department of Industrial
Engineering,
Tekirdag
Turkey
asagbas@nku.edu.tr

José María Sanz
University of Valencia
Polytechnic,
Departament of Statistics
Operation Research and
Applied Quality
Valencia
Spain